

Supporting information

Chirality variation from self-assembly to Ullmann coupling for the DBCh adsorbate on Ag(111) and Au(111)

Hongbing Wang,^{a, b} Jinping Hu,^{a, b} Zhaofeng Liang,^{*, c} Huan Zhang,^{a, b} Chaoqin

Huang,^{a, b} Lei Xie,^c Zheng Jiang,^{a, b, c} Han Huang,^d Fei Song^{* a, b, c}

*^a Shanghai Institute of Applied Physics, Chinese Academy of Sciences, Shanghai,
201204, China*

^b University of Chinese Academy of Sciences, Beijing, 10000, China

*^c Shanghai Synchrotron Radiation Facility, Shanghai Advanced Research Institute,
Chinese Academy of Sciences, Shanghai, 201204, China*

*^d School of Physics and Electronics, Central South University, Changsha, 410000,
China*

To whom the correspondence should be: liangzf@sari.ac.cn; songfei@sinap.ac.cn

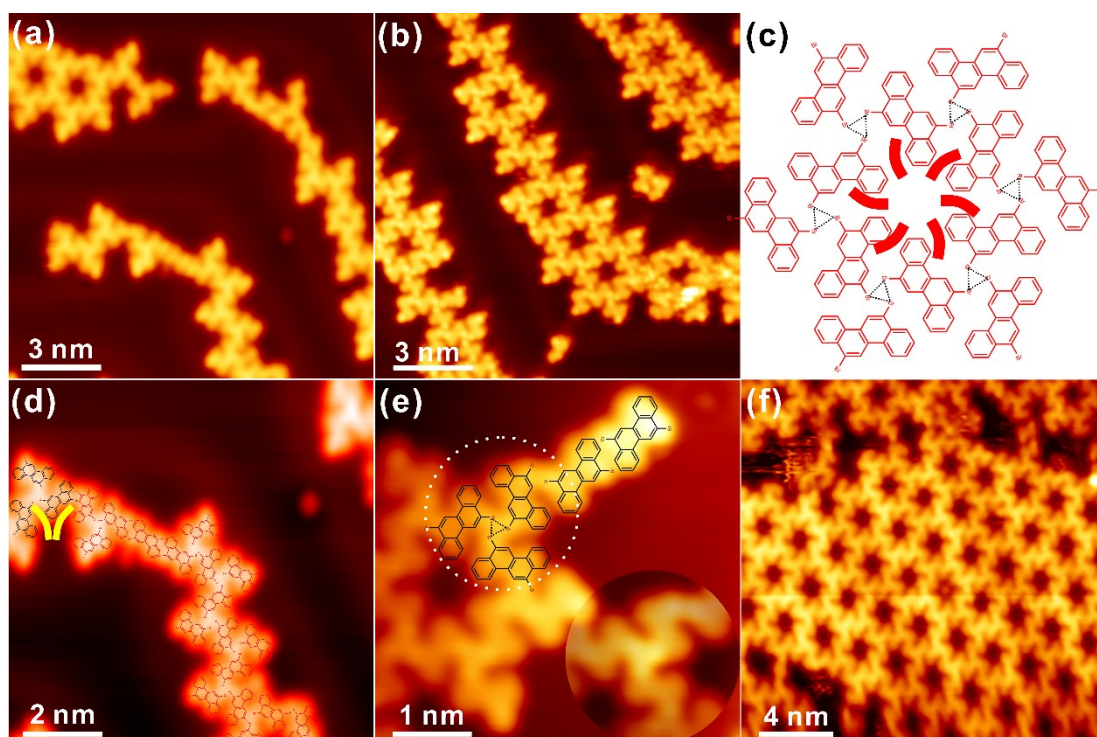


Fig. S1 (a) and (b) Zoom-in views of CW and ACW phases around the elbow site of the herringbone reconstruction. (c) The proposed structural configuration of the homochiral ACW phase. Halogen bonding motifs is indicated with black dashed lines. (d) Chain-shape structures formed before the appearance of hexamers on Au(111). As highlighted by the molecular model, *S* and *R* enantiomers can be packed in the same chain with a clear junction between CW and ACW phases. (e) High-resolution STM showing the arrangement of *R* chiral adsorbate with varying bonding motifs. (f) The ACW arrangement on Au(111) at the full coverage besides the CW phase in Figure 2a. Scanning parameters: $U_{\text{bias}}=-1.8 \text{ V}$, $I_t=0.2 \text{ nA}$.

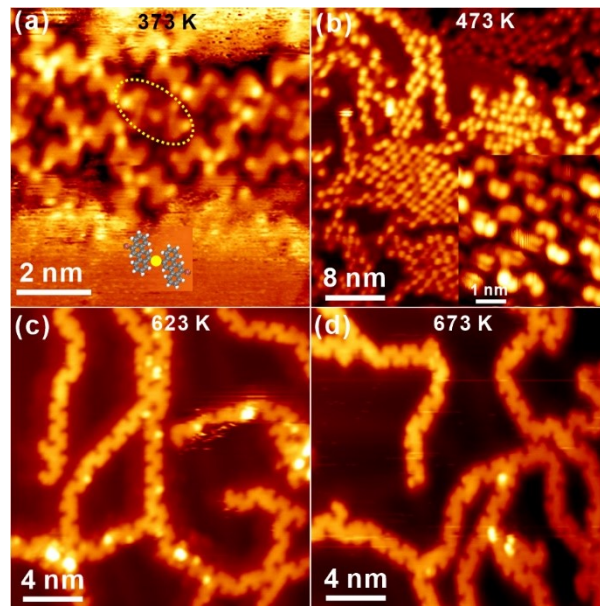


Fig. S2 (a) The formation of OM dimer inside collapsed hexagonal patterns on Au(111), in addition to the observed OM dimers in Figure 3a. (b) Annealing to 473 K induces the formation of ‘zig-zag’ chains over the whole surface and the high-resolution image shown inset. (c) The formation of planar polymer chain after annealing to 623 K in large area. (d) The robustness of polymer chains witnessed by sequential annealing to 673 K. Scanning parameters: $U_{\text{bias}}=-1.8$ V, $I_{\text{t}}=0.2$ nA.

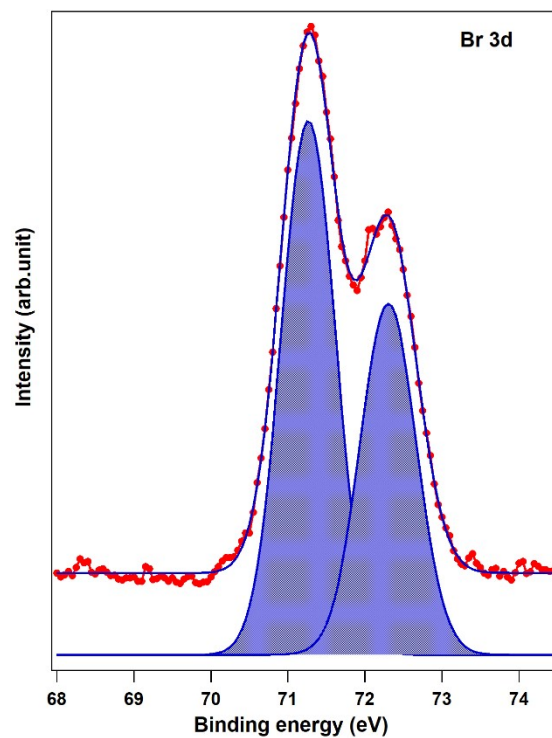


Figure S3. XPS recording of the Br 3d core level after the deposition of DBCh on Ag(111) held at RT. Fitted data (linear background subtracted, the Voigt function used for peak fitting) is presented

with blue curves. Clearly, there is only one pair of Br 3d peaks (the Br 3d_{5/3} and 3d_{3/2} doublet) resolved in the spectrum, which is assigned to the carbon-bound bromine species (C-Br) in DBCh molecules (Ref 35, 37 and 38 in the main text).

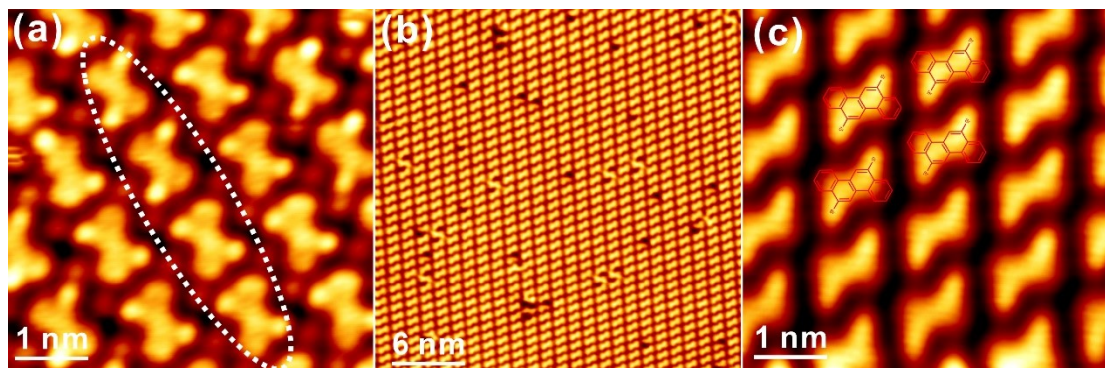


Fig. S4 The zoom-in view of the defective site on Ag(111) in correspondence to Figure 4a, where the chiral adsorbate of enantiomers is found in the same column. (b) Single domain of the unique DBCh enantiomer (*S*) without adsorption chirality on Ag(111). (c) The corresponding molecule-resolved STM with the molecular model overlaid. Scanning parameters: $U_{\text{bias}} = -1.6$ V, $I_t = 0.1$ nA.

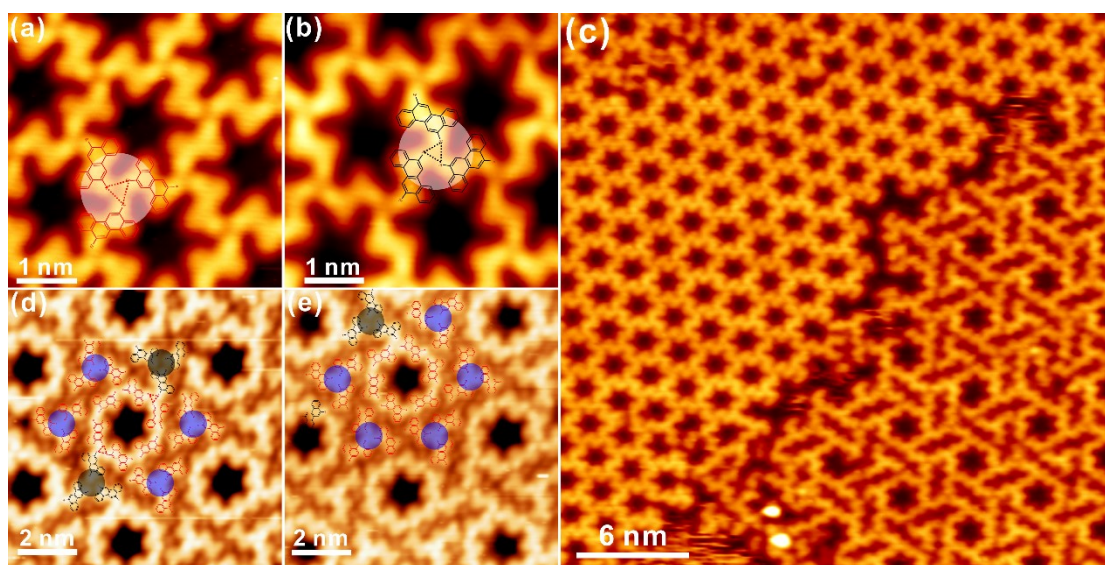


Fig. S5 (a) and (b) Zoom-in views of CW and ACW phases on Ag(111) in correspondence to Figure 5a. (c) Coexistence of the hexagonal phase and decorated hexagonal pattern. (d) and (e) 4 and 5 synthons with the same chirality are positioned around the inner hexamer besides observations in Figure 5f and 5g. Scanning parameters: $U_{\text{bias}} = -1.8$ V, $I_t = 0.1$ nA.

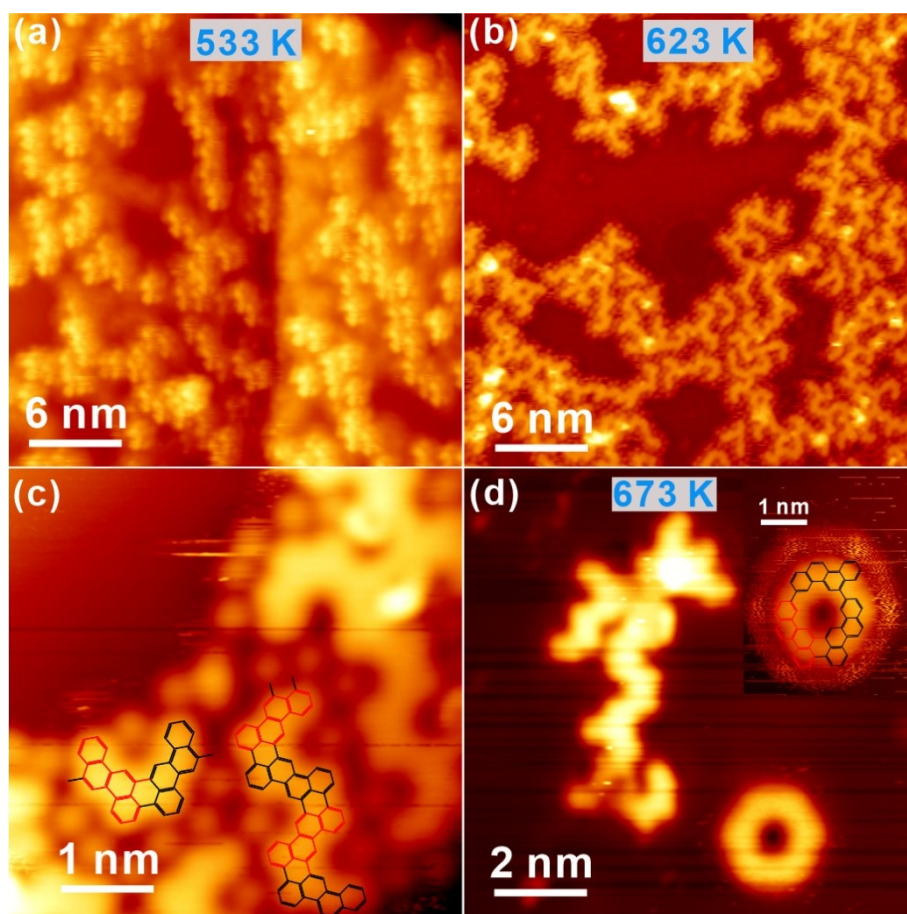


Fig. S6 (a) Structural chaos is observed on Ag(111) after annealing to 533 K. Localized oligomers are found over the whole surface. (b) Further annealing to 623 K induces the extended oligomers with the improved arrangement. Br adatoms are attracted on both sides of chains. (c) The zoom-in view with dimers and oligomers clearly identified in combination with the corresponding structural models. (d) Intensive annealing to 673 K results the desorption of polymers and the formation of closed ring structure. Scanning parameters: $U_{\text{bias}}=-1.5$ V, $I_t=0.1$ nA.